Comparison of Interatomic Potentials for Modeling Defects in Graphene Using Molecular Dynamics

M.A. Rozhkov[1,*] [ID] **, A.L. Kolesnikova[1,2]** [ID] **, A.E. Romanov[1,3]** [ID]

[1] Institute of Advanced Data Transfer Systems, ITMO University, Kronverksky Pr. 49, bldg. A, St. Petersburg 197101, Russia
[2] Institute for Problems in Mechanical Engineering RAS, V.O., Bolshoj pr., 61, St. Petersburg 199178, Russia
[3] Togliatti State University, Belorusskaya str. 14, Togliatti 445020, Russia

Article history	Abstract
	In this work, we tested the ability of classical interatomic potentials to describe the energy characteristics of defects of various dimensionality in graphene crystals. Brenner's Reactive Empirical Bond Order potentials (second generation REBO, AIREBO, AIREBO-M), Tersoff potentials, as well as BOP and LCBOP potentials were considered. The data obtained in this work using the molecular dynamics method was compared with literature data obtained using the density functional theory. It is noted that when modeling point and linear defects, the potentials of the REBO family and the LCBOP potential demonstrate the best agreement with the literature data. For modeling pseudo-graphene crystals, the best fit is demonstrated by the Tersoff B-N-C potential, which shows slightly overestimated energy values for linear and point defects, but most accurately describes the geometry of the crystal lattice. The potential of BOP demonstrates its inability to correctly model defect configurations with high densities of eight-member defect rings. When simulating four-member carbon defect rings, most potentials exhibit distortions in the crystal lattice that are not observed in the density functional theory calculations.

1. INTRODUCTION

The study of carbon materials has always been a broad area of research due to the very different combinations of possible characteristics of carbon polymorphs [1]. The most famous example is the comparison of graphite and diamond, which have diametrically opposed characteristics [2]. It is known that changes in the properties of a material can be achieved not only by changing its crystal lattice, transforming it from one polymorph to another, but also by introducing defects into the crystal lattice [3]. For example, embedding of grain boundaries into graphene can demonstrate an increase in electrical conductivity along this boundary by several orders of magnitude [4]. In this regard, the study of the influence of defect structure on the characteristics of materials is an important area of research in materials science.

One of the important criteria when analyzing crystal structure defects is the study of energy characteristics. Using these data, it is possible to predict possible changes in crystal structure under various external conditions: for example, the formation, migration, or interaction of defects in crystal lattice. Along with analytical methods, there is the molecular dynamics method, which is excellent for analyzing the dynamics of defects inside a crystal, which has proven itself well in this area [5,6]. The method is based on the use of the previously obtained interatomic interaction potential, which describes the dependence of the interaction forces between atoms depending on the distance. However, as practice shows, potentials are not universal—

---

they are developed to solve problems in a narrow area, adjusting the parameters of the potential to these tasks. When solving other problems, they can demonstrate a large error in the results obtained, instability of calculations, or give unphysical results [7]. All this imposes many restrictions on the use of interatomic interaction potentials and requires careful verification of applicability for solving a specific problem. In this regard, the purpose of this article is to study the dependence of the energy characteristics of defects of various dimensionality in graphene on the interatomic potentials used.

2. METHODS AND DESCRIPTION OF INTERATOMIC INTERACTION POTENTIALS

In this work, we use molecular dynamics simulation within the LAMMPS software package [8]. During the simulation, energy minimization was carried out using the conjugate gradient algorithm. The time step was chosen to be 0.1 fs. The simulation was carried out at 0 K using a Berendsen barostat, and periodic boundary conditions were applied to the model boundaries. To simulate crystals whose models were difficult to adapt to the use of periodic boundary conditions, the approach described in Ref. [9] was adopted: a large graphene sheet is used and the edges of the sheet are excluded from the calculation of the total energy to ignore the contribution of surface energy at the edges of the sheet. To visualize the results, the OVITO software package was used [10].

To model the formation energy of point defects, the following formula was utilized:

$$E_{defect} = E_{total} - E_{in}\frac{N_0 + n}{N_0},$$

where E_{total} is the energy of graphene crystal together with the defect, E_{in} is the energy of defect-free graphene, N_0 is the number of atoms in the initial ideal graphene lattice, n is the number of atoms that are added (or removed) after the formation of a defect relative to the initial crystal lattice.

To analyze linear defects, the energy of the defect in the crystal was found, similar to the approach for point defects, and then divided by the length of the defect. To analyze the energy of pseudo-graphene crystals, an approach was used to compare the energies per atom between a defective and an ideal graphene crystal.

The work compared several potentials. The potential of the second generation REBO has proven itself in the modeling of carbon materials and hydrocarbons [11]. It was then modified to the AIREBO potential [12], which complements the pair interaction of the REBO potential with two additional terms: the Lennard-Jones potential to describe long-range interactions, as well as the four-body potential, which describes twisting and bending by considering the

angles in the bonds between carbon atoms. The AIREBO-M potential [13] is a variation of the AIREBO potential in which the Lennard-Jones potential is replaced by a Morse potential. This variation shows better stability of calculations with increasing atomic density or at high pressure applied.

The Tersoff potential is a good and productive three-body potential that has proven itself for modeling a wide variety of systems. In this work, three implementations of the Tersoff potential were compared: the original potential for the Si-C system [14] (hereinafter Tersoff 1989), a modernized version of the previous Si-C potential, in which refinements were made for more accurate modeling of carbon materials [15] (in hereinafter Tersoff 2005), as well as the potential for the B-N-C system [16] (hereinafter Tersoff B-N-C), which was developed to simulate the contact of graphene and boron nitride.

The potential of the BOP species for the C-Cu system was also considered [17], which was developed for the contact of copper and various carbon allotropes. In particular, it was used to develop models of the mechanical and energy characteristics of graphite, diamond, carbon nanotubes and graphene, as well as models of graphene growth and the phase transition between graphite and diamond.

The BOP potential has a modification considering long-range interactions—LCBOP. Within the framework of this work, this potential of interatomic interaction for carbon crystals was considered [18]. In this potential, the parameters for short-range covalent bonds in graphite layers and long-range interactions between graphite layers are carefully selected.

3. RESULTS OF MODELING AND DISCUSSION

3.1. Point defects

To test the interatomic interaction potentials, the following point defects were simulated: vacancy (Fig. 1a), divacancy (Fig. 1b), dislocation (Fig. 1c) and Stone-Wales defect (Fig. 1d).

Table 1 shows the results of modeling the formation energy of the considered point defects, and provides data obtained using density functional theory (DFT) for comparison. As can be seen from the results obtained, good agreement between the values is obtained mainly for the family of REBO potentials (AIREBO, AIREBO-M and REBO), as well as for the LCBOP potential. The obtained models of the atomic configurations differ little from each other, i.e., there are no transformations into defects of a different geometry. This means that despite incorrect estimates of the energy of defect formation, calculations using the remaining considered potentials show an adequate atomistic structure of point defects in the graphene crystal lattice.
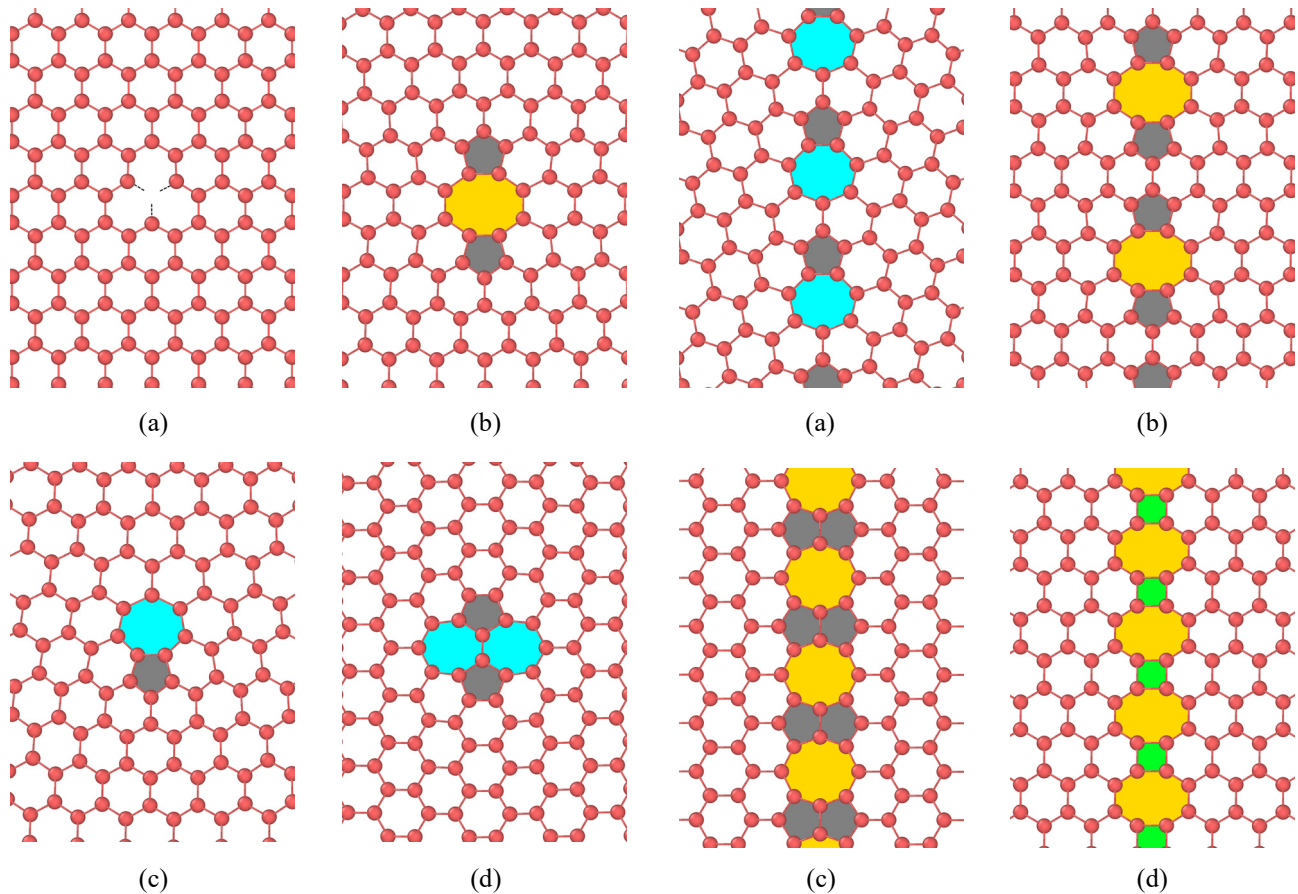
Fig. 1. Point defects in graphene lattice: vacancy (a), divacancy (b), dislocation (c), Stone-Wales defect (d).

Fig. 2. Grain boundaries and zero misorientation interfaces in graphene: GB 5-7A (a), ZMI 5-8-5A1 (b), ZMI 5-8-5D (c) and ZMI 4-8 (d).

Table 1. Formation energies (given in eV) of point defects.

Interatomic potential	$E_{vacancy}$	$E_{divacancy}$	$E_{dislocation}$	$E_{Stone-Wales}$
AIREBO (CH)	7.648	7.916	7.593	5.940
AIREBO-M (CH)	7.636	7.899	7.584	5.931
REBO (CH)	7.518	7.167	6.860	5.300
Tersoff (Si-C, 1989)	6.891	13.018	13.259	10.728
Tersoff (B-N-C)	0.519	9.534	8.740	6.140
Tersoff (Si-C, 2005)	5.878	11.474	11.189	9.024
BOP (C-Cu)	5.541	7.371	5.515	5.026
LCBOP (C)	7.593	7.164	7.121	4.972
DFT	7.4–7.8 [19–21]	7.8–8.7 [22–24]	7.8 [25]	4.8–5.2 [26]

Table 2. Energies (given in eV/Å) of intercrystallite interfaces.

Interatomic potential	E_{5-7A}	$E_{5-8-5A1}$	E_{5-8-5D}	E_{4-8}
AIREBO (CH)	0.457	0.954	0.679	1.113
AIREBO-M (CH)	0.456	0.951	0.677	1.104
REBO (CH)	0.401	0.847	0.593	0.963
Tersoff (Si-C, 1989)	0.894	1.548	1.583	2.261
Tersoff (B-N-C)	0.466	1.110	0.743	1.156
Tersoff (Si-C, 2005)	0.706	1.341	1.286	2.059
BOP (C-Cu)	0.401	0.852	1.337	–
LCBOP (C)	0.378	0.842	0.529	1.405
DFT	0.338 [25]	–	0.527 [28]	–

3.2. Linear defects

To compare the interatomic interaction potentials when modeling linear defects, we took a grain boundary (GB) model consisting of pentagonal and heptagonal carbon rings—GB 5-7A (Fig. 2a), as well as models of low-energy intergrain zero misorientation interfaces (ZMI) [27]: ZMI 5-8-5A1 (Fig. 2b), ZMI 5-8-5D (Fig. 2c) and ZMI 4-8 (Fig. 2d). The simulation results are presented in Table 2.

As can be seen from the results obtained, the energy values for the studied grain-grain interfaces and grain boundaries obtained using the REBO family potentials and the LCBOP potential are comparable to the data obtained using DFT. Among the family of Tersoff potentials,
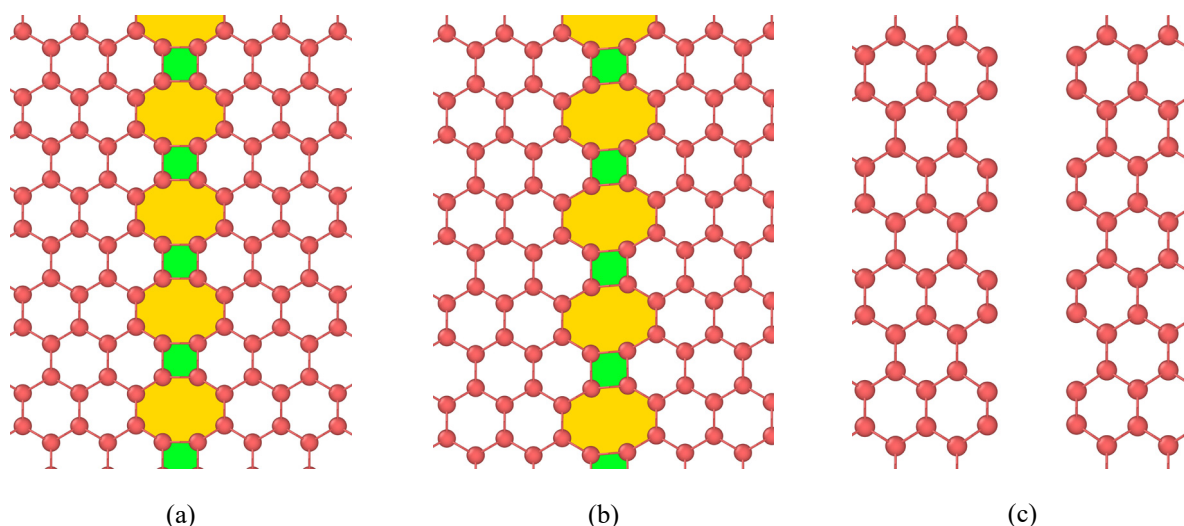
Fig. 3. Atomistic models of zero misorientation interface 4-8 obtained using different interatomic potentials: Tersoff B-N-C (a), AIREBO (b) and BOP (c).
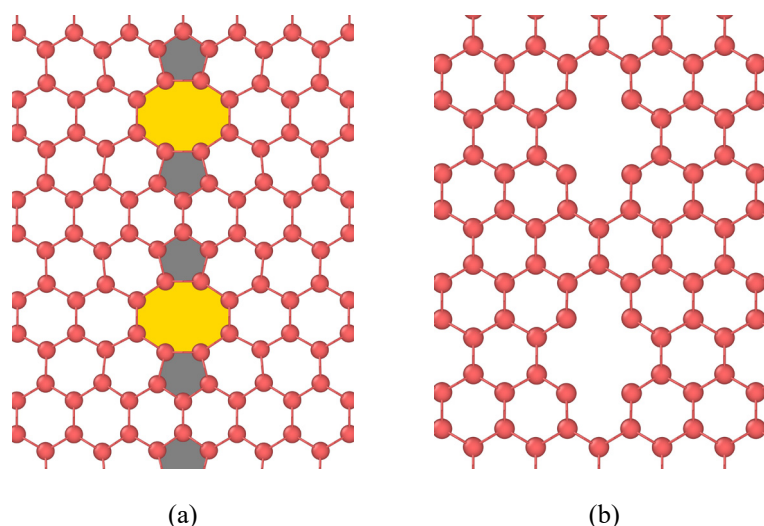
Fig. 4. Atomistic models of zero misorientation interface 5-8-5A1 obtained using different interatomic potentials: Tersoff B-N-C (a) and BOP (b).

which give overestimated values for all linear defects, one can highlight the implementation for the B-N-C system: the values, although higher than in the literature data, are relatively close to them. But more importantly, if we consider ZMI 4-8, then this potential shows the most regular atomistic structure compared to other potentials (see Fig. 3). If we take the calculations carried out using DFT [29], four-member carbon atomic rings should have a rectangular shape (see Fig. 3a). For all other potentials except the BOP potential, the four-member carbon rings have a parallelogram shape, and they also introduce distortions into the adjacent eight-member carbon rings (Fig. 3b). When calculating this atomistic model using the BOP potential, the crystal was separated into two parts at the interface (Fig. 3c). This potential shows a similar picture when modeling the ZMI 5-8-5A1 interface (see Fig. 4): the defective configuration

is destroyed as a result, and a large pore is formed in place of the defects (Fig. 4b). This suggests that this potential is poorly suited for modeling crystals with a high density of defects, as well as for modeling defects in the form of eight-member carbon rings.

3.3. Pseudo-graphene crystals

Pseudo-graphene crystals were taken as samples for modeling the two-dimensional distribution of defects in graphene: G5-6-7v2, G5-7v1, G5-6-8v2, G5-6-8v3, G5-6-8v4, G5-8v1 and G4-8v1 (see Fig. 5). These pseudo-graphenes were chosen because they are among the lowest energy crystals [30]. The names of pseudo-graphene crystals are taken from the classification proposed in Ref. [31].
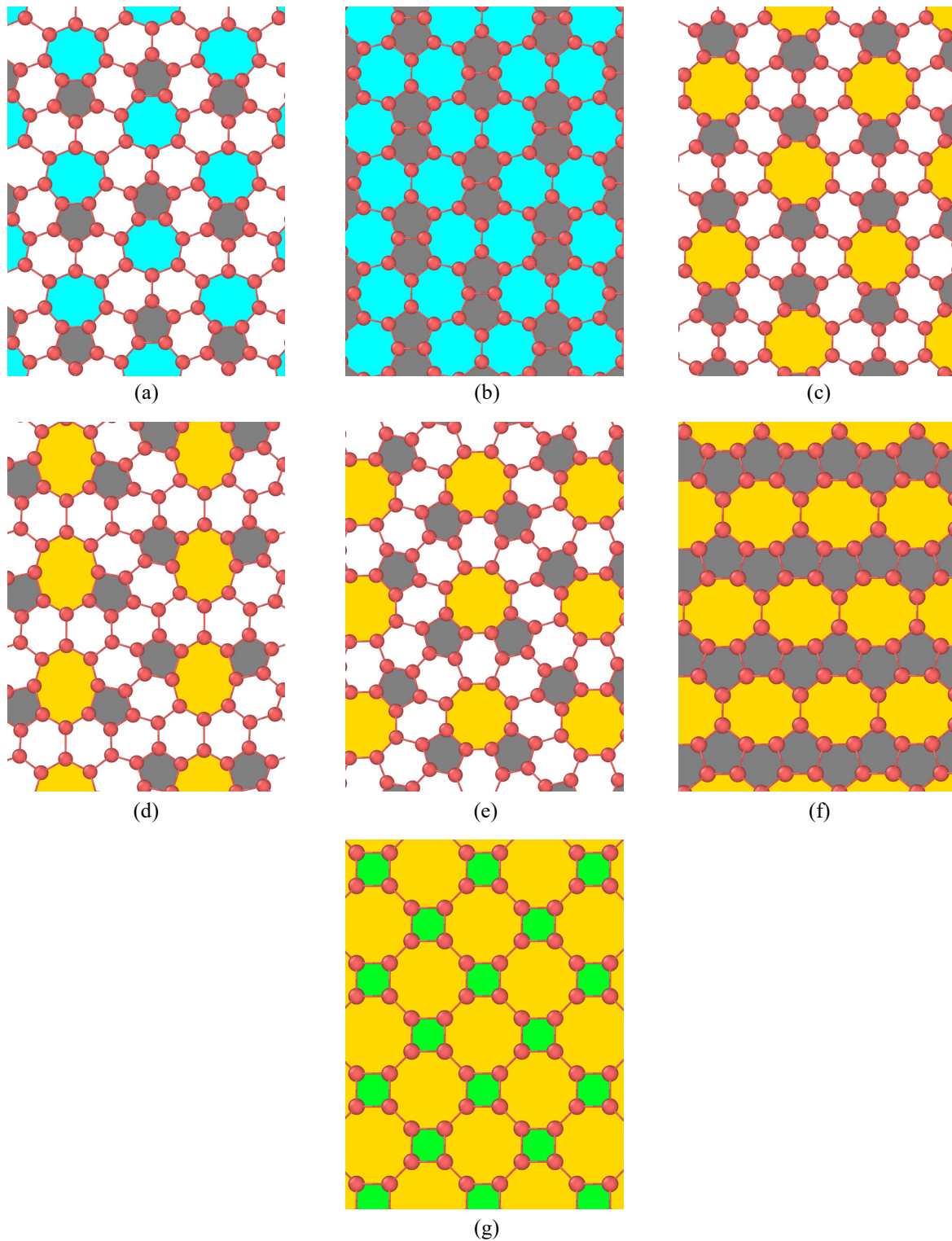
Fig. 5. Atomistic models of pseudo-graphene crystals: G5-6-7v2 (a), G5-7v1 (b), G5-6-8v2 (c), G5-6-8v3 (d), G5-6-8v4 (e), G5-8v1 (f) and G4-8v1 (g).

Table 3 shows the results of potential energy modeling for the considered pseudo-graphene crystals. The obtained energy values are given in eV per atom after comparison with graphene.

As can be seen from the results obtained, upon relative comparison with literature data, similar results were found in most cases by potentials of the REBO, Tersoff B-N-C and LCBOP family. If we talk about the correspondence of the geometry of atomistic models, then the Tersoff 2005 and Tersoff B-N-C potentials showed a good agreement. Thus, for modeling pseudo-graphene crystals, the Tersoff B-N-C potential showed the best results. Regarding other

Table 3. Energies (given in eV/atom) of pseudo-graphene crystals.

Interatomic potential	$E_{G5-6-7v2}$	E_{G5-7v1}	$E_{G5-6-8v2}$	$E_{G5-6-8v3}$	$E_{G5-6-8v4}$	E_{G5-8v1}	E_{G4-8v1}
AIREBO (CH)	0.276	0.374	0.332	0.458	0.393	0.522	0.979
AIREBO-M (CH)	0.275	0.373	0.331	0.457	0.392	0.521	0.977
REBO (CH)	0.248	0.330	0.296	0.400	0.352	0.463	0.878
Tersoff (Si-C, 1989)	0.551	0.857	0.754	0.811	0.833	1.249	2.060
Tersoff (B-N-C)	0.273	0.367	0.373	0.499	0.420	0.569	0.691
Tersoff (Si-C, 2005)	0.440	0.688	0.609	0.697	0.663	1.008	1.940
BOP (C-Cu)	0.261	0.427	0.555	0.543	0.579	1.156	1.531
LCBOP (C)	0.227	0.288	0.277	0.409	0.329	0.391	1.303
DFT	0.2 [32]	0.323 [33]	–	–	–	0.32 [34]	0.707 [33]

(a)   (b)
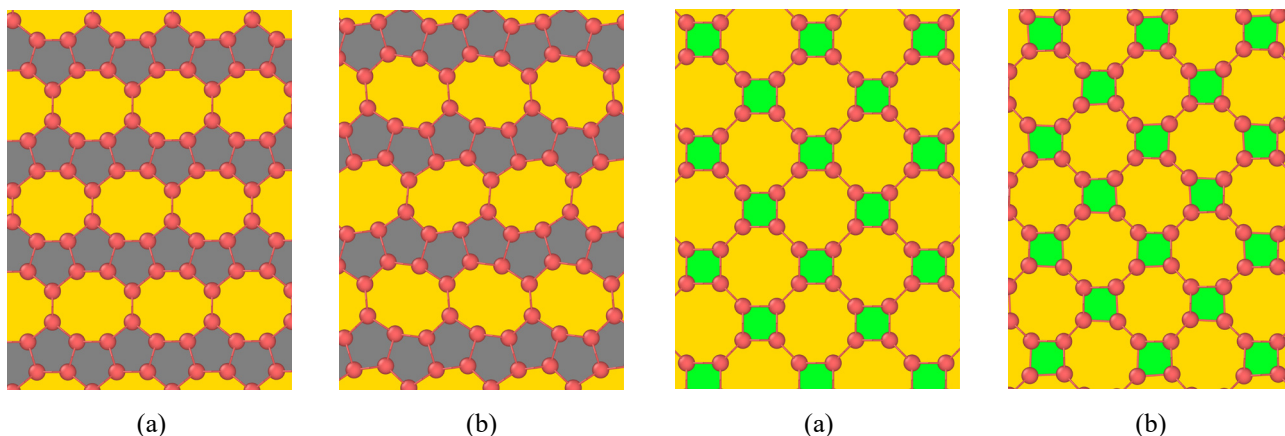
Fig. 6. Atomistic models of pseudo-graphene crystal G5-8v1 obtained using different interatomic potentials: Tersoff B-N-C (a) and Tersoff 1989 (b).
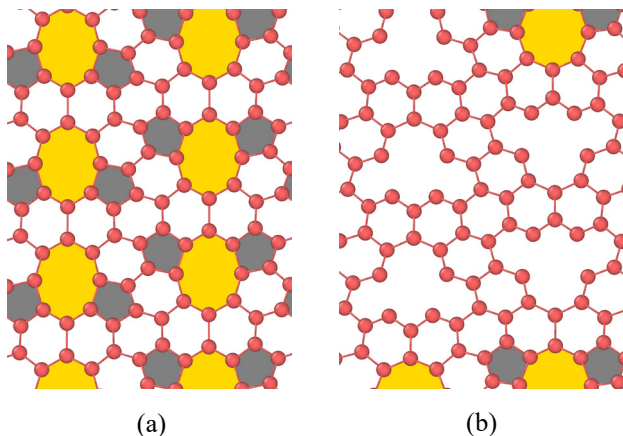
(a)   (b)

Fig. 7. Atomistic models of pseudo-graphene crystal G5-6-8v3 obtained using different interatomic potentials: Tersoff B-N-C (a) and BOP (b).

(a)   (b)

(c)   (d)

Fig. 8. Atomistic models of pseudo-graphene crystal G5-6-8v3 obtained using different interatomic potentials: Tersoff 2005 (a), LCBOP (b), AIREBO (c) and BOP (d).

potentials, for example, the Tersoff 1989 potential showed a mismatch in the pseudo-graphene crystal G5-8v1 simulation, bending defective carbon rings (see Fig. 6b). The remaining potentials showed results similar to the atomistic model given in Ref. [34]. The BOP potential, similar to previous results, showed an inability to simulate densely packed defects, turning the combination of two pentagonal

and one octagonal carbon ring into a large pore (see Fig. 7b).

In the simulation of G4-8v1 pseudo-graphene, only the models obtained using the Tersoff B-N-C and Tersoff 2005 potentials showed results (see Fig. 8a) consistent with the atomistic model obtained using DFT [33]. Similar to the situation, when simulating the ZMI 4-8 interface, the remaining potentials introduced distortions into the lattice, deforming the shape of regular squares and octagons: The LCBOP potential showed a slight distortion of the

crystal lattice (Fig. 8b), and the Tersoff 2005 and REBO family potentials showed strong distortions of the pseudographene lattice (Fig. 8c). The BOP potential, similar to previous results, transformed the defect configuration into large pores (Fig. 8d).

4. CONCLUSIONS

As a result, it was demonstrated that when modeling point and line defects, it is better to use the REBO family potentials and the LCBOP potential, which show the best agreement with the data obtained using DFT. In modeling pseudo-graphene crystals, the best agreement was found for the Tersoff B-N-C potential, which can also be applied to modeling linear defects with the limitation that it sometimes gives overestimated energies. This interatomic potential also showed the best agreement when compared with the crystal structure geometry obtained using DFT.

According to the results obtained, crystals with defects containing four- and eight-member rings cause difficulties in modeling for most potentials, despite the good convergence of their results for modeling defect-free graphene and other carbon allotropes.

As a possible option for achieving optimal results when modeling defects of any dimensionality in graphene crystals, the Tersoff B-N-C potential should be adjusted to obtain more accurate values of the formation energy of point and linear defects.

ACKNOWLEDGEMENTS

REFERENCES

[1] E.H. Falcao, F. Wudl, Carbon allotropes: beyond graphite and diamond, *Journal of Chemical Technology and Biotechnology*, 2007, vol. 82, no. 6, pp. 524–531.

[2] N. Mounet, N. Marzari, First-principles determination of the structural, vibrational and thermodynamic properties of diamond, graphite, and derivatives, *Physical Review B*, 2005, vol. 71, no. 20, art. no. 205214.

[3] F. Banhart, J. Kotakoski, A.V. Krasheninnikov, Structural defects in graphene, *ACS Nano*, 2011, vol. 5, no. 1, pp. 26–41.

[4] J. Lahiri, Y. Lin, P. Bozkurt, I.I. Oleynik, M. Batzill, An extended defect in graphene as a metallic wire, *Nature Nanotechnology*, 2010, vol. 5, no. 5, pp. 326–329.

[5] P.V. Polyakova, J.A. Baimova, Mechanical Properties of Graphene Networks under Compression: A Molecular Dynamics Simulation. *International Journal of Molecular Sciences*, 2023, vol. 24, no. 7, art. no. 6691.

[6] M.A. Rozhkov, A.L. Kolesnikova, I.S. Yasnikov, A.E. Romanov, Disclination ensembles in graphene, *Low Temperature Physics*, 2018, vol. 44, no. 9, pp. 918–924.

[7] I.V. Lebedeva, A.S. Minkin, A.M. Popov, A.A. Knizhnik, Elastic constants of graphene: Comparison of empirical potentials and DFT calculations, *Physica E: Low-dimensional Systems and Nanostructures*, 2019, vol. 108, pp. 326–338.

[8] LAMMPS Molecular Dynamics Simulator, *Electronic resource*, accessed 16.03.2024.

[9] M.A. Rozhkov, A.L. Kolesnikova, T.S. Orlova, L.V. Zhigilei, A.E. Romanov, Disclinated rings as structural units in MD simulation of intercrystallite boundaries in graphene, *Materials Physics and Mechanics*, 2016, vol. 29, no. 1, pp. 101–105.

[10] A. Stukowski, Visualization and analysis of atomistic simulation data with OVITO–the Open Visualization Tool, *Modelling and Simulation in Materials Science and Engineering*, 2009, vol. 18, no. 1, art. no. 015012.

[11] D.W. Brenner, O.A. Shenderova, J.A. Harrison, S.J. Stuart, B. Ni, S.B. Sinnott, A second-generation reactive empirical bond order (REBO) potential energy expression for hydrocarbons, *Journal of Physics: Condensed Matter*, 2002, vol. 14, no. 4, pp. 783–802.

[12] S.J. Stuart, A.B. Tutein, J.A. Harrison, A reactive potential for hydrocarbons with intermolecular interactions, *The Journal of Chemical Physics*, 2000, vol. 112, no. 14, pp. 6472–6486.

[13] T.C. O'Connor, J. Andzelm, M.O. Robbins, AIREBO-M: A reactive model for hydrocarbons at extreme pressures, *The Journal of Chemical Physics*, 2015, vol. 142, no. 2, art. no. 024903.

[14] J. Tersoff, Modeling solid-state chemistry: Interatomic potentials for multicomponent systems, *Physical Review B*, 1989, vol. 39, no. 8, pp. 5566–5568.

[15] P. Erhart, K. Albe, Analytical potential for atomistic simulations of silicon, carbon, and silicon carbide, *Physical Review B*, 2005, vol. 71, no, 3, art. no. 035211.

[16] A. Kınacı, J.B. Haskins, C. Sevik, T. Çağın, Thermal conductivity of BN-C nanostructures, *Physical Review B*, 2012, vol. 86, no. 11, art. no. 115410.

[17] X.W. Zhou, D.K. Ward, M.E. Foster, An analytical bond-order potential for carbon, *Journal of Computational Chemistry*, 2015, vol. 36, no. 23, pp. 1719–1735.

[18] J.H. Los, A. Fasolino, Intrinsic long-range bond-order potential for carbon: Performance in Monte Carlo simulations of graphitization, *Physical Review B*, 2003, vol. 68, no. 2, art. no. 024107.

[19] I.A. Pašti, A. Jovanović, A.S. Dobrota, S.V. Mentus, B. Johansson, N.V. Skorodumova, Atomic adsorption on graphene with a single vacancy: systematic DFT study through the periodic table of elements, *Physical Chemistry Chemical Physics*, 2018, vol. 20, no. 2, pp. 858–865.

[20] L. Wang, X. Zhang, H.L. Chan, F. Yan, F. Ding, Formation and healing of vacancies in graphene chemical vapor deposition (CVD) growth, *Journal of the American Chemical Society*, 2013, vol. 135, no. 11, pp. 4476–4482.

[21] K. Iyakutti, E. Mathan Kumar, R. Thapa, R. Rajeswarapalanichamy, V.J. Surya, Y. Kawazoe, Effect of multiple defects and substituted impurities on the band structure of graphene: a DFT study, *Journal of Materials Science: Materials in Electronics*, 2016, vol. 27, pp. 12669–12679.

[22] R.G. Amorim, A. Fazzio, A. Antonelli, F,D. Novaes, A.J. da Silva, Divacancies in graphene and carbon nanotubes, *Nano Letters*, 2007, vol. 7, no. 8, pp. 2459–2462.

[23] A.A. El-Barbary, R.H. Telling, C.P. Ewels, M.I. Heggie, P.R. Briddon, Structure and energetics of the vacancy in graphite, *Physical Review B*, 2003, vol. 68, no. 14, art. no. 144107.

[24] A.V. Krasheninnikov, P.O. Lehtinen, A.S. Foster, R.M. Nieminen, Bending the rules: Contrasting vacancy energetics and migration in graphite and carbon nanotubes, *Chemical Physics Letters*, 2006, vol. 418, no. 1–3, pp. 132–136.

[25] O.V. Yazyev, S.G. Louie, Topological defects in graphene: Dislocations and grain boundaries, *Physical Review B*, 2010, vol. 81, no. 19, art. no. 195420.

[26] L. Li, S. Reich, J. Robertson, Defect energies of graphite: Density-functional calculations. *Physical Review B*, 2005, vol. 72, no. 18, art. no. 184109.

[27] A.L. Kolesnikova, M.A. Rozhkov, I. Hussainova, T.S. Orlova, I.S. Yasnikov, L.V. Zhigilei, A.E. Romanov, Structure and energy of intercrystallite boundaries in graphene, *Reviews Advanced Materials Science*, 2017, vol. 52, no. 1/2, pp. 91–98.

[28] A.R. Botello-Méndez, X. Declerck, M. Terrones, H. Terrones, J.C. Charlier, One-dimensional extended lines of divacancy defects in graphene, *Nanoscale*, 2011, vol. 3, no. 7, pp. 2868–2872.

[29] A.W. Robertson, G.D. Lee, K. He, E. Yoon, A.I. Kirkland, J.H. Warner, The role of the bridging atom in stabilizing odd numbered graphene vacancies. Nano Letters, 2014, vol. 14, no. 7, pp. 3972–3980.

[30] A.E. Romanov, M.A. Rozhkov, A.L. Kolesnikova, Disclinations in polycrystalline graphene and pseudo-graphenes. Review, *Letters on Materials*, 2018, vol. 8, no. 4, pp. 384–400.

[31] N.D. Abramenko, M.A. Rozhkov, A.L. Kolesnikova, A.E. Romanov, Structure and properties of pseudo-graphenes. Review, *Reviews on Advanced Materials and Technologies*, 2020, vol. 2, no. 4, pp. 9–26.

[32] Z. Wang, X.F. Zhou, X. Zhang, Q. Zhu, H. Dong, M. Zhao, A.R. Oganov, Phagraphene: a low-energy graphene allotrope composed of 5–6–7 carbon rings with distorted dirac cones, *Nano Letters*, 2015, vol.15, no. 9, pp. 6182–6186.

[33] A.N. Enyashin, A.L. Ivanovskii, Graphene allotropes, *Physica Status Solidi B*, 2011, vol. 248, no. 8, pp. 1879–1883.

[34] C.P. Tang, S.J. Xiong, A graphene composed of pentagons and octagons, *AIP Advances*, 2012, vol. 2, no. 4, art. no. 042147.

Сравнение потенциалов межатомного взаимодействия для моделирования дефектов в графене с помощью метода молекулярной динамики

М.А. Рожков[1], А.Л. Колесникова[1,2], А.Е. Романов[1,3]

[1] Институт перспективных систем передачи данных, Университет ИТМО, Кронверкский пр., д. 49, лит. А, Санкт-Петербург, 197101, Россия

[2] Институт проблем машиноведения РАН, В.О., Большой пр., д. 61, Санкт-Петербург, 199178, Россия

[3] Тольяттинский государственный университет, Белорусская ул., д. 14, Тольятти, 445020, Россия

Аннотация. В настоящей работе мы проверили способность классических межатомных потенциалов описывать энергетические характеристики дефектов различной размерности в кристаллах графена. Рассмотрены потенциалы реактивного эмпирического порядка связи Бреннера (REBO второго поколения, AIREBO, AIREBO-M), потенциалы Tersoff, а также потенциалы BOP и LCBOP. Данные, полученные в данной работе методом молекулярной динамики, сравнивались с литературными данными, полученными с помощью DFT. Отмечено, что при моделировании точечных и линейных дефектов наилучшее совпадение с литературными данными демонстрируют потенциалы семейства REBO и потенциал LCBOP. Для моделирования кристаллов псевдографена лучше всего подходит потенциал Tersoff B-N-C, который показывает несколько завышенные значения энергии для линейных и точечных дефектов, но наиболее точно описывает геометрию кристаллической решетки. Потенциал BOP демонстрирует неспособность правильно моделировать конфигурации дефектов с высокой плотностью восьмичленных дефектных колец. При моделировании четырехчленных углеродных дефектных колец большинство потенциалов проявляют искажения кристаллической решетки, которые не наблюдаются в расчетах DFT.

Ключевые слова: графен; молекулярная динамика; дефекты; псевдо-графены